

Semi-automatic Segmentation of MRI Brain Metastases Combining Support Vector Machine and Morphological Operators

Gloria Gonella¹, Elisabetta Binaghi¹, Paola Nocera^{2,3} and Cinzia Mordacchini²

¹*Department of Theoretical and Applied Science, Insubria University, Varese, Italy*

²*C. S. Health Physics, ASST dei Sette Laghi, Varese, Italy*

³*Department of Physics, University of Milan, Milan, Italy*

Keywords: MRI Brain Tumour Segmentation, Support Vector Machine, Morphological Operators.

Abstract: The objective of this study is to develop a semi-automatic, interactive segmentation strategy for efficient and accurate brain metastases delineation on Post Gadolinium T1-weighted brain MRI images. Salient aspects of the proposed solutions are the combined use of machine learning and image processing techniques, based on Support Vector Machine and Morphological Operators respectively, to delineate pathological and healthy tissues. The overall segmentation procedure is designed to operate on a clinical setting to reduce the workload of health-care professionals but leaving to them full control of the process. The segmentation process was validated for in-house collected image data obtained from radiation therapy studies. The results prove that the allied use of SVM and Morphological Operators produces accurate segmentations, useful for their insertion in clinical practice.

1 INTRODUCTION

Magnetic Resonance Imaging (MRI) segmentation has a central role in the assessment of a wide spectrum of brain pathologies, in clinical settings. It allows identification and delineation of tissues, thanks to the high spatial resolution and contrast of images, and due to enhanced signal differentiation (Greenberg et al., 1999).

In radiation therapy (RT), a precise and accurate segmentation of MR brain metastases is important to the planning of best-case treatments. In this context automated methods of MRI brain segmentation represent a valuable improvement to rough manual detection and delineation, by supporting human operators with varying degrees of automation, in tracing the boundaries of pathological tissues and by automatically providing accurate quantitative measures used in further stages (Kaus et al., 2001; Withey and Koles, 2008; Charron et al., 2018; Sharp et al., 2014). Even though fully automated segmentation algorithms have the advantage of computing results in less time and low effort, semi-automated, interactive methods could be preferable in principle, allowing to incorporate useful prior knowledge from the experts and then, making the overall segmentation procedure more accurate and controllable (Joe et al., 1999;

Pedoia et al., 2015). In the last years many methods have been developed for the automatic segmentation of MRI brain tumors. The proposed techniques make use of a single image or multispectral pattern and are supervised or unsupervised (Gordillo et al., 2013; Bauer et al., 2013).

Even though a large number of techniques have been proposed in the literature, their application to brain metastases has received a lot less attention so far. Yan Liu et al., (2016) propose an automatic segmentation strategy for metastatic brain tumour delineation on contrast-enhanced T1-weighted (T1c) MR image for stereotactic radiosurgery (SRS) applications. The strategy combines several techniques such as clustering and regional active contour technique. A fully automated method is proposed by Charron et al., (2018). In their study, an existing 3D convolutional neural network (DeepMedic) is adapted to detect and segment brain metastases on multimodal MRI.

Despite the relevant results recently obtained, there is a need for further studies to investigate novel approaches able to provide robust solutions and fulfil spatial accuracy and reproducibility requirements.

The objective of this study is to develop a semi-automatic, interactive segmentation strategy for efficient and accurate brain metastases delineation on

Post Gadolinium T1-weighted (T1c) brain MRI images. The salient aspects of the solutions proposed are the combined use of machine learning and image processing techniques, based on Support Vector Machine (SVM) (Vapnik, 1995) and Morphological Operators (Gonzalez and Woods, 2018) respectively, to delineate pathological and healthy tissues. The overall segmentation procedure is designed to operate in a clinical setting to reduce the workload of health-care professionals but leaving to them full control of the process. It is then conceived semi-automatic, but requiring limited user interaction in an attempt to facilitate the insertion in current clinical practice.

The segmentation process was validated for in-house collected image data obtained from RT studies, where manually segmented images are also provided by a team of experts.

2 METHODS

The overall segmentation procedure is hierarchically structured in three phases:

- Volume-of-interest (VoI) specification
- Supervised Classification based on SVM
- Segmentation Refinement based on Morphological Operators

2.1 VoI Specification

The underlying assumption is that segmentation when limited to a significant sub-region, could have performances significantly better in terms of speed and accuracy than if the segmentation were applied to the entire scene.

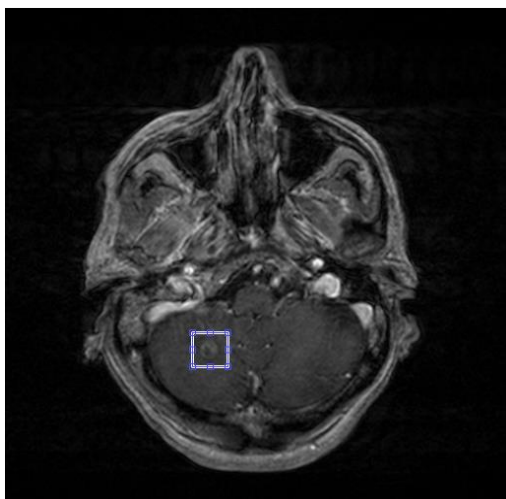


Figure 1: Source Slice of a T1c volumetric MR scan with the corresponding VoI slice.

In this step, a user specifies a volume of interest (VoI) by drawing a rectangular region on one slice of the input volume and selecting first and last slices in such a way that the entire pathological area is bounded within the specified parallelepiped (see Figure 1).

2.2 Supervised Classification of Pathological and Healthy Tissues

In the second phase, a supervised classification is applied to the selected sub-image.

Among the variety of automated classifiers well-suited for biomedical image segmentation, we choose the SVM model (Vapnik, 1995; Suykens et al., 2002).

In our previous works, we deal with MRI brain tumor segmentations using several methods selected from states of the art classifiers in the field of MRI segmentation. In particular, we investigated the use of Fuzzy connectedness and Graph Cut for glial tumor segmentation (Pedoia et al., 2015; Binaghi et al., 2016) and SVM for meningioma and edema segmentation (Binaghi et al., 2018). Fuzzy Connectedness and Graph Cut methods are interactive asking experts to provide accurate initialization information. Results obtained by these methods were accurate but strongly influenced by the prior knowledge provided by the users or by ancillary methods. In RT domain, where a large number of images are needed to be handled, they can be laborious and time-consuming. We have shown that SVM allows complete delineation of meningioma and edema tissues and accurate volume estimation by processing both volumetric and non-volumetric imagery in a few minutes, without requiring manual selection of example voxels.

Performances obtained were good confirming the results obtained in other studies (Bauer et al., 2011).

Proceeding from these results, in the present work we have considered SVM a potentially valuable tool for brain metastases segmentation in RT daily care. In this preliminary study, the in-house collected image dataset is limited and the SVM model could optimize the balance between accuracy and demand of the number of training data.

Multidimensional input patterns are composed of Post Gadolinium T1-weighted (T1c) voxel intensities and corresponding textural and contextual features extracted from the MR scan.

SVM classifier performs a binary hard categorization labelling voxels as Metastasis (M) and Healthy tissue (H). Different types of kernels are tested such as linear, quadratic, cubic, fine-medium-coarse gaussian. Given the results obtained, we configured the SVM as soft-margin least square (LS)

model with linear kernel. The trained SVM classifier receives in input patterns, in the form of vectors of measured features and assigns labels to corresponding T1c MR elements.

Different sets of features have been proposed in the literature, selected in the function of the MRI channels used and the classifiers adopted (Gordillo et al., 2013; Bauer et al., 2013). On the basis of our experience, in addition to image intensities from the T1c MR scan, we consider features describing quantitatively neighbour relationships and texture (Tuceryan and Jain, 1998). Contextual and textural features have been analysed systematically in order to determine the combination that is most appropriate for the current classification task.

In particular, several configurations of the segmentation procedure have been experimented initially providing input only intensity values of central voxel and of neighbour voxels.

Different neighbourhoods have been considered including incrementally neighbours along voxel faces, corners and edges up to a maximum of 26 voxels. In a second step an enlarged feature set has been considered adding textural features to the best neighbourhood configuration. The following set of features has been finally selected:

- intensities from T1c scan
- first order texture features, mean, variance, skewness, kurtosis and entropy
- intensities in 26 neighbourhood voxels

The features have been normalized to have zero mean and unit variance.

During the training phase, the SVM learns an approximation for the true input–output relationship based on a given training set of examples constituted by N input–output pairs $\{x_i, y_i\}, i = 1, \dots, N$, where x_i is the feature vector of length equal to 32 and $y_i \in \{M, H\}$ is a supervised label denoting the membership in the metastasis or healthy class.

Several strategies are conceived to build the appropriate training set during the learning stage. All proposed training sets have been analysed systematically in the experimental evaluation phase in order to determine the combination that is most appropriate for the classification task (see Section 3).

2.2.1 SVM Classifier

To make the work self-contained we briefly outline the basic concepts of SVM adopted in the proposed segmentation strategy. SVM is a classification algorithm based on kernel methods (Vapnik, 1995; Schoelkopf and Smola, 2002) map the input patterns

into a high dimensional feature space. Classes which are non-linearly separable in the original space can be linearly separated in the higher dimensional feature space.

Let $\{(x_i, y_i)\}$ be a supervised training set of elements for a two-class classification problem, with $x_i \in X \subseteq R^n$ and $y_i \in \{-1, 1\}$. Considering the case of linearly separable data, the solution to the classification problem consists in the construction of the decision function:

$$f(x) = \text{sgn}(g(x)) \text{ with} \quad (1)$$

$$g(x) = w^t x + b \quad (2)$$

that can correctly classify an input pattern x not necessarily belonging to the training set.

SVM classifier defines the hyperplane that causes the largest separation between the decision function values for the “borderline” examples from the two classes. Mathematically, this hyperplane can be found by minimizing the cost function:

$$J(W) = \frac{1}{2} \|W\|^2 \quad \text{subject to} \quad (3)$$

$$W^T X_i + b \geq +1 \text{ for } y_i = +1 \quad (4)$$

or

$$W^T X_i + b \leq -1 \text{ for } y_i = -1 \quad (5)$$

The extension to the nonlinear classification is based on the function $g' = W^T \varphi(X) + b$ in which the non-linear operator $\varphi(\cdot)$ is introduced.

In this case the SVM cost function to be minimized is

$$J(W, \xi) = \frac{1}{2} \|W\|^2 + C \sum_{i=1}^l \xi_i \quad \text{subject to} \quad (6)$$

$$y_i (w^t \varphi(X_i) + b) \geq +1 - \xi_i \text{ with} \quad (7)$$

$$\xi_i \geq 0, i = 1, 2, \dots, l$$

Suykens (Suykens et al., 2002) proposed a new formulation of SVM by adding a LS term in the original formulation of the cost function. This modification significantly reduces the computational complexity.

2.3 Segmentation Refinement based on Morphological Operators

Recent studies propose the allied use of SVM with post-processing and/or regularisation procedures to ensure spatial consistency in classification results (Bauer et al., 2011). In our context, after the segmentation, if the tumour area presents necrosis

and inhomogeneity, small holes within the tumour mass may be classified as healthy tissues and several isolated elements in the background area may be classified as tumour. Our strategy includes a procedure based on the use of Morphological Operators to refine the segmented masks in an attempt to reduce omission and commission errors and making the segmented tumour area more compact.

For each selected slice, Opening and Closing Operators with spherical shapes are applied consequently. The Opening Operator removes from the binary input image all the connected components that have a lower number of pixels than a set value and outputs a new binary image. The Closing Operator closes holes present in the image and returns the closed binary image. Three different tests were performed, using for all a disk-shape structuring element, aimed to tune parameters values of the Morphological Operators and decide the order of application. In the first test, only the opening morphological operator (Open) was applied by varying the radius; in the second test, only the morphological closing operator (Close) was applied, varying the radius; in the third test, both operators were applied in a different sequence. The best result was the third test, where the opening morphological operator with a radius of 5 was first applied and then the closing operator with a radius equal to 10.

3 EXPERIMENTS

The segmentation method was experimented on a dataset of 20 patients with a total of 25 pathologies to be segmented. Data are composed of T1c volumetric MR scans. Volumes are acquired using a 3D sequence characterized by 0,9 mm isotropic voxels, the pixel spacing of 0,47 mm and the slice thickness of 2,67 mm.

We developed case-specific, intra-case analysis and inter-case analysis. In case-specific analysis both training and test sets were obtained from the reference masks of the same VoI. In inter-case analysis training and test data are extracted from VoIs of different MR scans.

Accuracy of segmentation results is assessed by comparing the spatial distribution of the masks obtained by the automated segmentation with that of the masks obtained through a manual segmentation of the T1c images. The agreement between reference and automated maps is measured in terms of Dice (DSC) (Dice, 1945), Precision (P) and Recall (R) indexes (Olson and David, 2008). The DSC index has

been used broadly in the field of segmentation as a measure of spatial overlap and P and R indexes allow to measure under- and over-estimations (Bouix et al. 2007).

Several experiments have been conducted for both intra- and inter-case analysis distinguished by the criteria for selecting training and test samples from the VoIs under study. Experiments and accuracy assessments computed according to cross-validation scheme are detailed below.

3.1 Experiments for Intra-case Analysis

Experiment 1a: training and test data are extracted from the reference masks of the same VoI (intra-case analysis) and built by randomly selecting elements in the proportion of 70% and 30% respectively. An equal number of elements labelled M and H was considered. The number of contour elements belonging to class M was increased to facilitate recognition.

Experiment 2a: training and test sets are obtained as above, but by limiting the random selection within a region of 8 pixels wide, built around the contour of the tumour reference masks. The underlying assumption for this strategy lies in the fact that metastases have little extensions and a high level of heterogeneity occurs in the internal part of the pathology due to the presence of necrosis. In this context, an accurate delineation can be achieved by identifying the partial contour region, subsequently filled by the support of Morphological Operators.

Table 1: Dice (DSC), Precision (P), Recall (R) values obtained for Experiment 1a and Experiment 2a over all 25 cases under study.

		Experiment 1a	Experiment 2a
DSC	Mean	0.808	0.878
	Var	0.008	0.003
	Min	0.549	0.757
	Max	0.908	0.963
P	Mean	0.824	0.884
	Var	0.006	0.003
	Min	0.648	0.749
	Max	0.927	0.963
R	Mean	0.796	0.873
	Var	0.012	0.003
	Min	0.476	0.764
	Max	0.923	0.963

Table 1 shows the numerical results obtained for *Experiment 1a* and *Experiment 2a* in terms of DSC, P and R indexes. SVMs trained according to *Experiment 2a* slightly prevail with a DSC value computed over all 25 cases equal to 0.878. P and R values highlight a significant reduction of omission and commission errors.

3.2 Experiments for Inter-case Analysis

Two types of experiments for inter-case analysis have been conducted distinguished by an increasing level of heterogeneity of the training set provided in input to the SVM classifier. The random selection of training elements was limited to contour regions of tumour reference masks; the reason for this choice lies in the fact that this strategy prevailed in the intra-case analysis.

Experiment 1b: in this experiment, SVMs are trained on data from one case and tested on all the cases under study; in this way, we investigate the generalisation power of the SVM when training data present a minimum level of heterogeneity. 25 SVMs are trained with training elements extracted from the selected VoI, according to *Experiment 2a* and tested on all the VoIs under study. Results obtained by the best configuration when processing the 25 cases are shown in Table 2. To isolate the contribution of Morphological Operators within the overall segmentation procedure, accuracy values obtained with and without the use of them are computed.

Table 2: Dice (DSC), Precision (P), Recall (R) values obtained by the segmentation procedure configured for Experiment 1b with and without the use of Morphological Operators (MO) and tested on the overall 25 cases under study.

		SVM	SVM+MO
DSC	Mean	0.701	0.693
	Var	0.011	0.035
	Min	0.462	0
	Max	0.844	0.897
P	Mean	0.747	0.696
	Var	0.026	0.047
	Min	0.437	0
	Max	0.997	0.997
R	Mean	0.737	0.769
	Var	0.035	0.057
	Min	0.410	0
	Max	0.983	0.990

Experiment 2b: training elements are extracted from a set of VoIs selected from cases well segmented in intra-case analysis. Several configurations have been considered obtaining 120 SVMs trained on different sets of VoIs, according to the strategy described in *Experiment 2a*, and tested on all the 25 VoI under study. The accuracy obtained with and without the use of Morphological Operators are computed as shown in Table 3.

Table 3: Dice (DSC), Precision (P), Recall (R) values obtained by the segmentation procedure configured for Experiment 2b with and without the use of Morphological Operators (OM) and tested on the overall 25 cases under study.

		SVM	SVM+MO
DSC	Mean	0.653	0.660
	Var	0.008	0.028
	Min	0.390	0
	Max	0.770	0.820
P	Mean	0.681	0.641
	Var	0.017	0.025
	Min	0.278	0
	Max	0.968	0.881
R	Mean	0.710	0.762
	Var	0.026	0.035
	Min	0.482	0
	Max	0.955	0.976

In general, results obtained in *Experiment 1b* are better than those obtained in *Experiment 2b*. Looking at values in Table 2 in more detail, we found that performances obtained by the application of Morphological Operators are worse on average.

However, when studying individual cases, we have noticed that under-estimation and over-estimation errors occur systematically when the pathology occupies a very small volume (under the 100 elements) and is inserted in a highly heterogeneous context. An example is illustrated in Figure 2 where a slice (Slice 1) with a remarkable small metastasis is shown. The refinement accomplished by the Morphological Operators deletes all the true positive elements identified by the SVM classifier. On the contrary, the segmentation masks of the larger pathological area in the slice (Slice 2) shown in Figure 3, indicate that the segmentation strategy benefits from the allied use of SVM and Morphological Operators. Table 4 lists the numerical results of the cases illustrated in Figure 2 and 3.

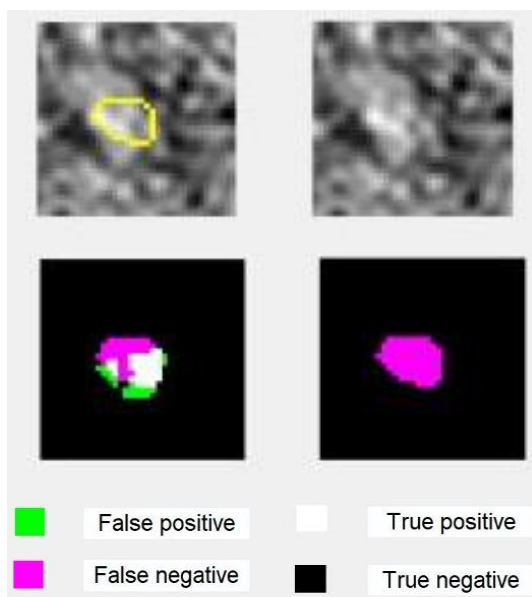


Figure 2: First row, from left to right: crop of a source slice (Slice 1) of T1 MR Volume with superimposed the contour of metastasis reference mask (dimension: 83 elements), Slice of the corresponding VoI; second row from left to right: Segmentation mask produced by SVM, refinement by the Morphological Operators.

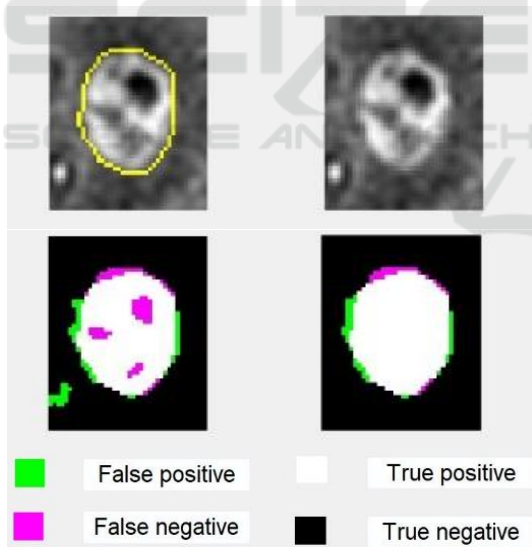


Figure 3: First row, from left to right: crop of a source slice (Slice 2) of T1 MR Volume with superimposed the contour of metastasis reference mask (dimension: 644 elements), Slice of the corresponding VoI; second row from left to right: Segmentation mask produced by SVM, refinement by the Morphological Operators.

Automatic segmentations were evaluated qualitatively through visual inspection. The complete strategy including the combined use of SVM and

Morphological Operators have been judged satisfactory. The limitations of the segmentation procedure, inherent to specific cases, as illustrated above, are considered acceptable and manageable with interactive phases devoted to manual refinements of the automated results.

Table 4: Dice (DSC), Precision (P), Recall (R) values obtained by the segmentation procedure when processing slices in Figure 2 and 3.

		DSC	Precision	Recall
Slice 1	SVM	0.556	0.656	0.482
	SVM+MO	0	0	0
Slice 2	SVM	0.885	0.898	0.873
	SVM+MO	0.940	0.926	0.953

4 CONCLUSIONS

The objective of this study was to develop a semi-automatic image segmentation strategy for metastases segmentation in MR brain images. The strategy was tested on a preliminary collected data set. The results prove that the allied use of SVM and Morphological Operators produces segmentation sufficiently accurate for their insertion in clinical practice. Future work contemplates the acquisition of new data with which to perform a more significant interpatient analysis and then to develop a more robust evaluation. Moreover, the availability of a wider set of data will allow-developing a comparative analysis with other promising segmentation techniques, such as the Convolutional Neural Network, the use of which is constrained to the collection of huge data sets.

REFERENCES

Bauer, S., Nolte, L.P., Reyes, M., 2011. ‘Fully automatic segmentation of brain tumor images using support vector machine classification in combination with hierarchical conditional random field regularization.’ In: *Medical image computing and computer-assisted intervention: MICCAI*, Berlin, Springer, 14, 354-61.

Bauer, S., Wiest, R., Nolte, L.P., Reyes, M., 2013. ‘A survey of MRI-based medical image analysis for brain tumor studies.’ *Physics in medicine and biology*, 58(13), R97-R129.

Binaghi, E., Padoia, V., Balbi, S., 2016. ‘Collection and fuzzy estimation of truth labels in glial tumour segmentation studies.’ *Computer Methods in Biomechanics and Biomedical Engineering: Imaging and Visualization*, 4 (3-4), 214-228.

Binaghi, E., Padoia, V., Balbi, S., 2018. ‘Meningioma and peritumoral edema segmentation of preoperative MRI

- brain scans.' *Computer Methods in Biomechanics and Biomedical Engineering: Imaging and Visualization*, 6 (4), 362-370.
- Bouix, S., Martin-Fernandez, M., Ungar, L., Nakamura, M., Koo, M.S., McCarley, W.R., Shenton, M., 2007. 'On Evaluating Brain Tissue Classifiers without a Ground Truth.' *NeuroImage*, 36, 1207-1224.
- Charron, O., Lallement, A., Jarnet, D., Noblet, V., Clavier, J.B., Meyer, P., 2018. 'Automatic detection and segmentation of brain metastases on multimodal MR images with a deep convolutional neural network.' *Computers in Biology and Medicine*.
- Dice, L.R., 1945. 'Measures of the amount of ecologic association between species.' *Ecology*, 26(3), 297-302.
- Gonzalez, R., Woods, R., 2018. *Digital Image Processing*, Pearson-Prentice Hall, 519-566.
- Gordillo, N., Montseny, E., Sobrevilla, P., 2013, 'State of the art survey on MRI brain tumor segmentation.' *Magn Reson Imaging*, 31(8), 1426-38.
- Greenberg, H., Chandler, W., Sandler, H., 1999. *Brain Tumors*, Oxford University Press, Oxford.
- Joe, B., Fukui, M., Meltzer, C., Huang, S.Q., Day, R., Greer, P., Bozik, M., 1999. 'Brain Tumor Volume Measurement: Comparison of Manual and Semiautomated Methods1.' *Radiology*, 212(3), 811-6.
- Kaus, M., Simon, P., Warfield, K., Nabavi, A., Peter, M., Black, M., Jolesz, F., Kikinis, R., 2001. 'Automated segmentation of MRI of brain tumors.' *Radiology*, 218, 586-591.
- Liu, Y., Stojadinovic, S., Hryushko, B., Wardak, Z., Lu, W., Yan, Y., Jiang, S., Timmerman, R., Abdulrahman, R., Nedzi, L., Gu, X., 2016. 'Automatic metastatic brain tumor segmentation for stereotactic radiosurgery applications.' *Physics in medicine and biology*, 61, 8440-8461.
- Olson, D.D., David, L., 2008. *Advanced Data Mining Techniques*, 1st Edition, Springer.
- Pedoaia, V., Balbi, S., Binaghi, E., 2015. 'Fully Automatic Brain Tumor Segmentation by using Competitive EM and Graph Cut.' In: *International Conference on Image Analysis and Processing*, Genova, Italy.
- Sharp, G., Fritscher, K., Pekar, V., Peroni, M., Shusharina, N., Veeraraghavan, H., Yang, J., 2014. 'Vision 20/20: Perspectives on automated image segmentation for radiotherapy.' *Medical physics*, 41(5), 050902.
- Schoelkopf, B., Smola, A., 2002. *Learning with kernels: support vector machines, regularization, optimization, and beyond*, MIT Press.
- Suykens, J.A.K., Van Gestel, T., De Brabanter, J., De Moor, B., Vandewalle, J., 2002. *Least Squares Support Vector Machines*. World Scientific Publishing Co., Singapore.
- Tuceryan M., Jain A., 1998. *Texture analysis Inc. River Edge*, NJ: World Scientific Publishing.
- Vapnik, V.N., 1995. *The Nature of Statistical Learning Theory*, Springer-Verlag, New York.
- Withey, D.J., Koles, Z.J., 2008. 'A review of medical image segmentation: Methods and available software.' *International Journal of Bioelectromagnetism*, 10, 125-14.